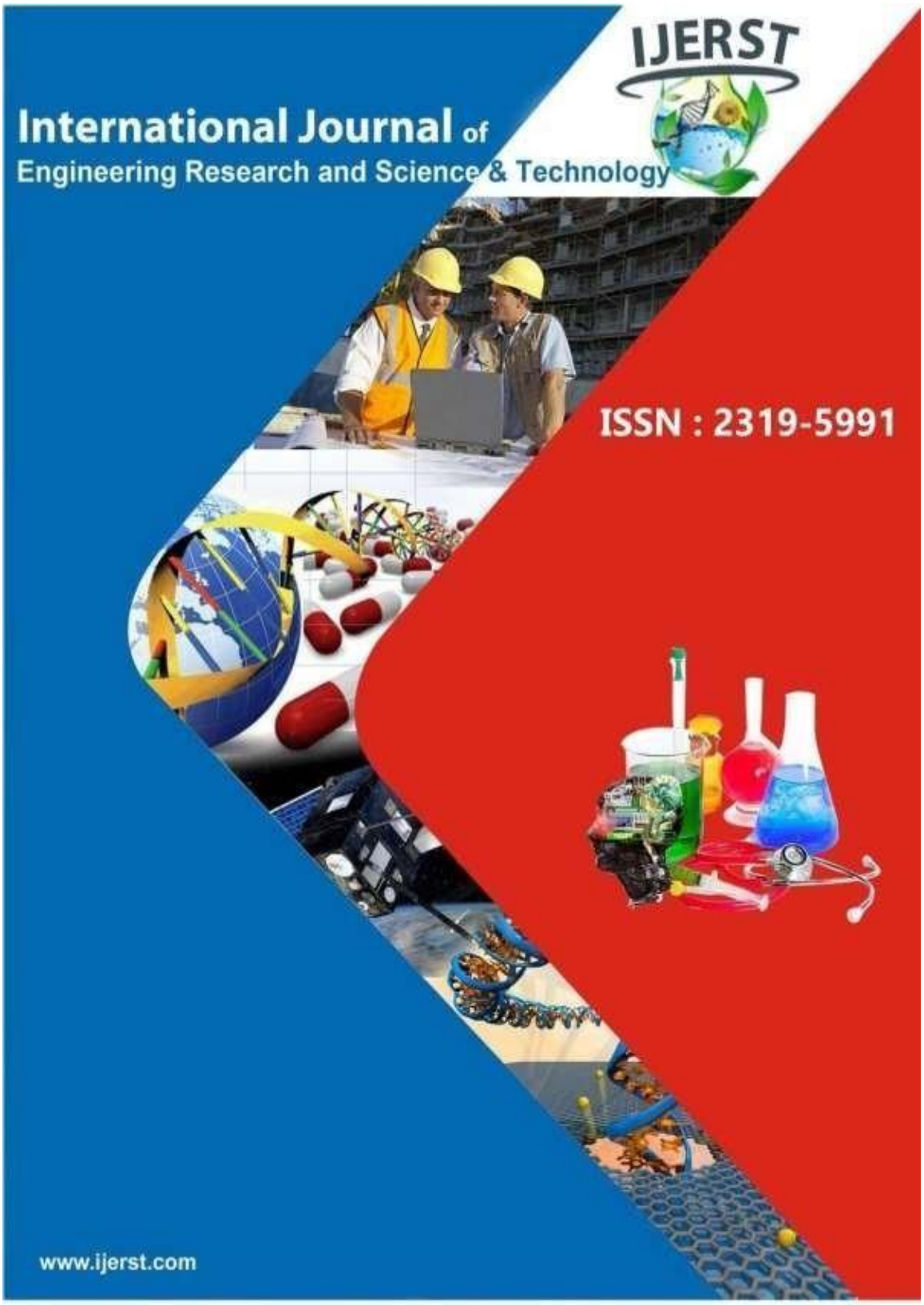

Email: editor@ijerst.com or editor.ijerst@gmail.com

ISSN 2319-5991 www.ijerst.com

Vol. 15, Issue.4, Dec 2019

A DESIGN AND ANALYSIS OF GAS TURBINE BLADE PROFILES USING DIFFERENT MATERIALS

[1]R.Narmada,[2]Illandula Venu
[12]Assistant Professor
Department Of Mechanical Engineering
Sree Chaitanya College of Engineering, Karimnagar

ABSTRACT:
Right now, one of the most effective sources of turbo machinery is gas turbines. Numerous industries, including manufacturing, aircraft, homes, and small businesses, may benefit from this technology. The selection of materials, turbine rotor blade vibration management, and blade shapes are all difficult tasks for gas turbine engines. These parameters have a major impact on stress deformation and structural performance. Analysis has been done on the overall heat flow, the directional distortions of the turbine blades, and the thermal inaccuracy that results from the heat and centrifugal stresses interacting. Furthermore, thermal loading is the cause of the temperature flow. To determine which material is best for a turbine blade, the performance of three different materials—Inconel 718, titanium T6, and SS316—is tested.

Key words: Study state, gas turbine blade Analyses of thermal and transient heat

1.0 INTRODUCTION

Gas turbines convert thermal energy obtained from the combustion of fuel in pressure gas and high temperatures into mechanical energy to drive electric generators **[1]** The engine of a gas turbine consists of three main parts, namely compressor, combustion system, and turbine **[2]** Components in the combustion system have a significant role in ensuring reliable operation in various air/fuel ratios and loads. Conditions of hot section components such as nozzles, burners, and blades exposed to hot gas coming out of the combustion system are very vulnerable to failure **[3].** The first stage blades in the turbine are considered very critical in hot gas path inspection. The most common failure mechanism modes in the nozzle and blade are fatigue, creep, erosion, and corrosion **[4]**. The first stage blade in a gas turbine function as a guide of hot gas supplied from the combustion chamber towards the turbine blade so that the blade experiences high heat pressure **[5]** Blades in turbines are usually made of nickel superalloys, coated with a thermal barrier **[6]** Gas turbines are the primary generators of energy in each of these experiments. Due to the high efficiency of gas turbines, they were chosen as the best option for this application. Three major components make up a simple gas-turbine: compressor, combustor, and turbine. Fuel and compressed air are combined and burned in a gas turbine that runs on the Brayton cycle principle. In order to generate power, the hot gas is expanded by turning a turbine.

Gas turbine:

Gas turbine engines convert the chemical energy of the fuel into mechanical energy, which can be expressed as shaft power or kinetic energy. Power production gas turbines are gas turbines specifically designed to produce electricity. The gas turbines on an airplane transform the fuel's potential energy into motion. Several parts of the engine collaborate to convert the energy stored in the fuel into the shaft power or propulsion force that moves the engine.

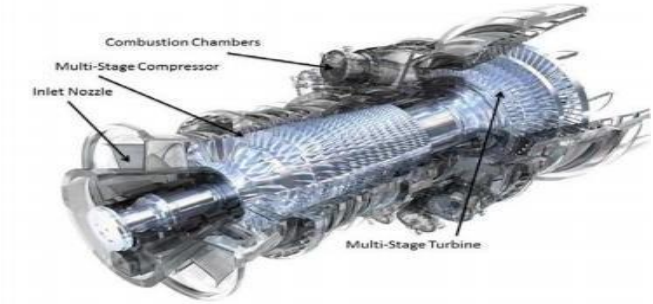

Figure 1: Gas turbine

ISSN 2319-5991 www.ijerst.com

Vol. 15, Issue.4, Dec 2019

Gas turbines convert combustion energy into heat by compressing the working gas (air). The working gas is subjected to rising temperatures and pressures. Working gas energy is converted into rotating blade energy by means of gas-blade interaction in the engine. Both types of gas turbines can be shown in the diagram below. There is an open cycle (which is internal) and a closed cycle (external type). The combustor and the turbine are the most crucial components of both compressors.

Gas turbine blade:

Turbine blades in gas turbines or steam turbines are made up of many smaller parts. The blades are what actually collect energy from the superheated, super pressed gas that the combustor produces. In order to function reliably in such extreme conditions, gas turbines frequently require exotic materials like superalloys and a wide variety of cooling technologies. These may be broken down into internal and external cooling, as well as thermal barrier coatings on the blades individually. For both steam and gas turbines, blade fatigue is a common cause of failure.

Figure 2: Turbine Blade

Applications of Gas Turbine:

- **Land Applications:** Central power stations, Industrial and Industrial.
- **Space Applications:** Turbo jet and Turbo prop.
- Marine application

Objectives:

- To study the gas turbine blade geometry
- A three-axis CNC machine was used to optimize the turbine blade, and different tools were used to manufacture it dimensionally.
- The Gas turbine blade design in done by using NX 12.0 and Analysis is done by ANSYS 2020R1(Inconel 625)
- To the gas turbine blade analyze with ANSYS 2022R1 (study state and transient thermal)

2.0 LITERATURE REVIEW

L.Umamaheswararao et al **[7]** have investigated the stress distribution and temperature distribution on gas turbine blade and have stated in paper titled "Design and analysis of a gas turbine blade by using FEM". In this paper the first stage rotor blade of a gas turbine has been analyzed for structural, thermal analysis using ANSYS (Finite Element Analysis Software). The material used for the blade was specified as INCONEL 718. P.V. Krishnakanth et al. **[8]** have summarized the design and analysis of Gas turbine blade in paper titled "Structural & Thermal Analysis of Gas Turbine Blade by Using F.E.M" in which CATIA V5 is used for design of solid model of the turbine blade with the help of the spline and extrudes options, ANSYS 11.0 software is used analysis of F.E. Barhm Abdullah Mohamad et al. **[9]** have worked on paper with title "Failure analysis of gas turbine blade using finite element analysis" related to failure analysis of the turbine blade of a gas turbine engine 9E GE type, installed in a certain type of simple systems consisting of the gas turbine driving an electrical power generator. Murali. K et al **[10]** have worked on the first stage rotor blade of the gas turbine in the paper titled with "Design and Fatigue Analysis of Turbine Rotor Blade by Using F.E.M". The first stage rotor blade of the gas turbine is Analysed for the static and thermal stresses resulting from the tangential, axial and centrifugal forces. Sindhu N L, Dr. N Chikkanna **[11]** In the present work the first stage rotor blade of a two-stage gas turbine has been Analyzed for static structural, steady state thermal, modal and high cycle fatigue using ANSYS 17. An attempt has been made to investigate the effect of temperature and induced stresses on the turbine blade.

3.0 RESEARCH METHODOLOGY

The aerospace engines have been the driving force behind the majority of the advancements in gas turbine technology. These engines were developed with a focus on maximizing reliability, performance, number of starts, and flexibility across the whole flight envelope. The utilization of high aspect ratio compressor blades and the optimization of pressure ratio and turbine firing temperature to

ISSN 2319-5991 www.ijerst.com

Vol. 15, Issue.4, Dec 2019

produce maximum work output per unit flow have traditionally been regarded as standards for aircraft engine performance. The industrial gas turbine has historically prioritized durability over other factors, resulting in a design that is less than optimal in terms of performance under stress. Industrial gas turbines can operate in low-temperature, high-pressure environments. A turbine is a device used to generate fluid flow, and its turbine rotor is turned by an agent that generates heat, typically an exhaust gas stream, gaseous byproducts of chemical reactions, or compressed gas. The key advantages of gas turbines are their portability, small size, great efficiency in energy conversion, straightforward build, and dependable performance.

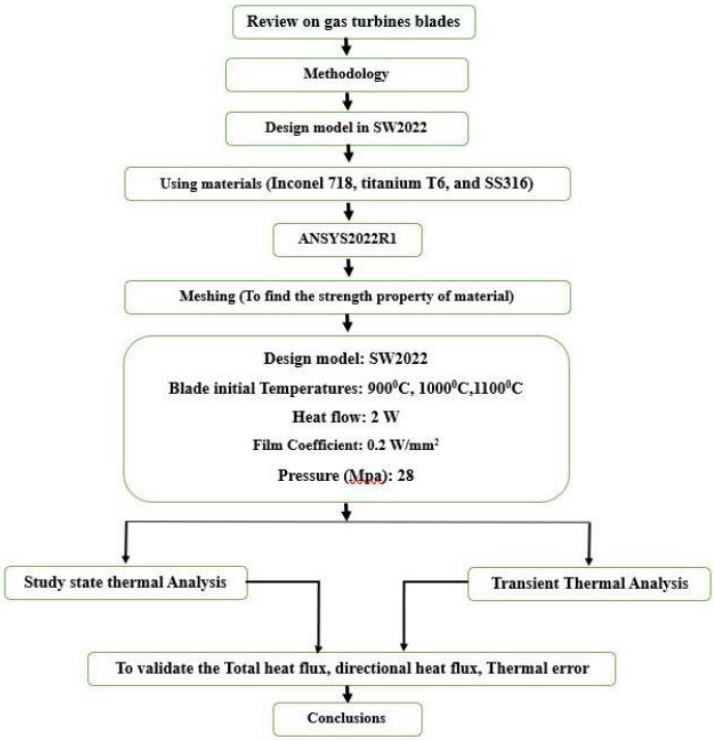

Figure 2: Design flow chart

Using materials:

The most important requirement for the gas turbine blade is to have high creep resistance at a higher temperature using different types blade materials in those analysis

Table 1: Gas turbine blade using different Material properties

Engineering Properties	Inconel 718	Titanium -T6	SS 316
Density (g/cc)	8.19	4.5	7.98
Thermal expansion coefficient (µm/m.°C)	13	7.14	17.2
Melting temperature (ºC)	1350	1725	1100
Young's modulus (Gpa)	204	100	190
Ultimate tensile strength (MPa)	965	1070	480
Poisson's ratio	0.29	0.36	0.3

INTRODUCTION TO NX 12.0

NX 12 delivers a number of feature editing and creation enhancements that drive productivity improvements. For example, you can now see the feature section direction when creating, editing, or replacing features. You now have the option to retain or delete child features when deleting features. This gives you more control over how your features is linked, and makes it easier to change or update your model.

ISSN 2319-5991 www.ijerst.com

Vol. 15, Issue.4, Dec 2019

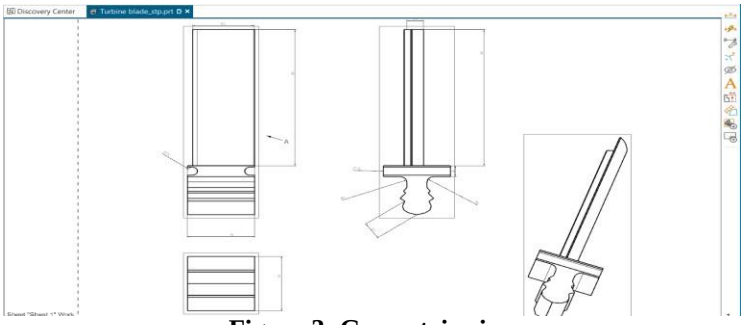

Figure 3: Geometric view

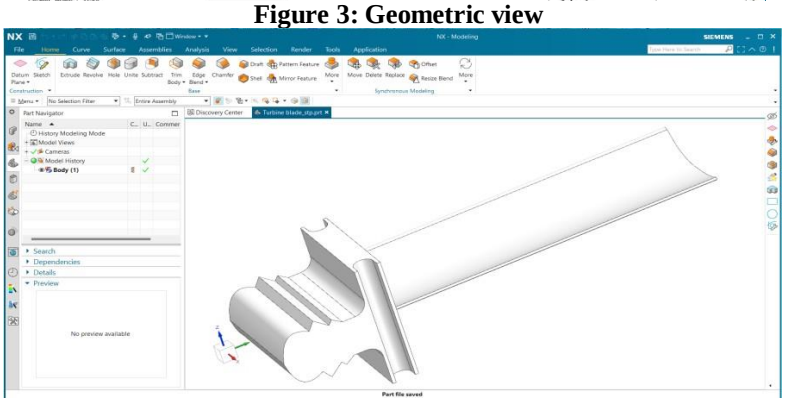

Figure 4: Gas turbine blade

Turbine blades

There are many methods of inspection of turbine blades, each of which may be used until all is inspected to a certain extent.

TBC Processing Methods

TBCs and EBCs are both types of coating materials frequently used as defense mechanisms for CMCs on components found in aerospace vehicles. CMCs are lighter and are able to endure higher temperatures than metallic materials do at 200 C. In dry air surfaces, protective silica forms which provide stability for long-term situations with temperatures of up to 1300 ˚C. However, the layer silica on the surface responds violently to surface recession in combustion conditions where moisture is present For CMC to work effectively in a hard and complex aircraft operating environments, a security system is therefore very important

VISUAL INSPECTION

As the name suggests, this type of check is a visually conducted preliminary examination, whether by inspection or by sight.

1. Bore scope: An engine component, such as turbine blades, can be examined using this equipment. With a flexible bore scope, the optical tube is adjustable so that it may be adjusted in various directions to find the component being inspected.

2. Magnifying glass: The blade may be examined with a loupe after disassembly, to see whether the blades are deformed and cracked.

Liquid Penetrating Testing

This approach includes the application of a fluorescent dye to the region to be investigated, and then highlights the points that are damaged or flawed. Until the paint or penetration can be applied on the turbine blade, all pollutants which can obstruct or fill the cracks on the blades' Depending on their size and composition, cracks and damaged regions may require more or less time for the penetrator to make its way inside. The next step is to remove the surplus dye from the blade.

Magnetic Particle Testing

It uses an induced magnetic force to reveal the defective areas on the blade surface. Indirect and direct magnetization of the component can be carried out. As the stream is applied through the blade, a magnetic field is created around it and a magnetic field is then applied from the outside to the blade. After any flaw in the blade has been magnetised, the magnetic flux will be released. The iron particles

ISSN 2319-5991 www.ijerst.com

Vol. 15, Issue.4, Dec 2019

are applied to the surface, and then the leakage is attracted. Any aggregation of iron particles in some areas indicates the defect in this position and necessary steps can be taken to repair this defect.

Eddy Current Inspection

Eddy current testing is a type of electromagnetic testing that employs electromagnetic induction to locate flaws in conductors. By passing an alternating current, the driver sets off the fields, the magnitude of which grows and shrinks as the current changes from maximum to minimum.

Laser Cutting Turbine Blade Different Operations:

Gas turbines are the rare synthesis of traditional heavy engine architecture and state-of-the-art development technology. Not only the entire turbine but also each blade is a technological marvel that blends high accuracy and efficiency. The shape of blades in a gas turbine varies and each undergoes extremely high operating stress. At 1,400 ° C,

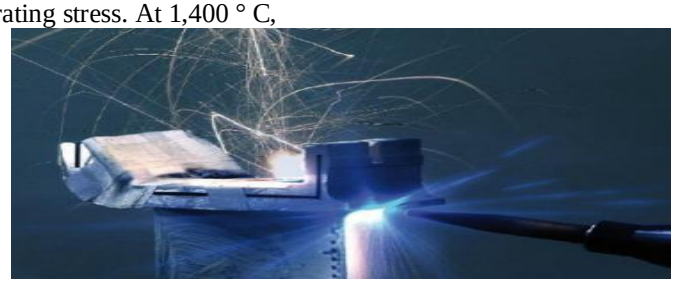

Figure 5: Turbine blade during laser drilling

The Laser systems for these deep penetration boxes (up to 25 mm) with pulse length are worked in the 1 mm range for these cylindrical holes at 15–90 ° C on curved blade surfaces. Moreover, most of the exit holes are created so as to allow the film to cool down.

Laser Drilling:

The number of cooling holes in turbine motors has risen considerably with the increased developments in laser process and control technology. Laser piercing enables the machining in a wide variety of materials in both very small and precise hole sizes and directions. These holes may be tapered or formed to improve the quantity, direction and cooling properties of the blade. One element with one setup can drill hundreds or thousands of cooling holes.

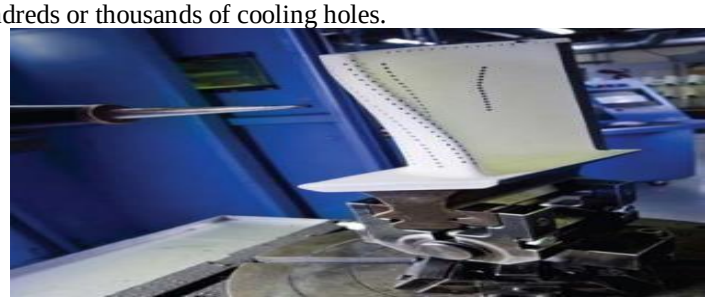

Figure 6: Laser drilling turbine blade

Cylindrical holes:

Melting and vaporising the material because of the absorption of energy from a concentrated laser beam is how most laser drillers of 0,8 mm diameter 0.0 hole in a 5 mm gap in turbine engine components work. Laser boiling pulse systems, the pulse length of which is determined by the system's overall parameters and is typically milliseconds for boiling turbine blades.

Figure 7: Gas turbine blade with about cooling holes, half of which have shaped exit holes.

ISSN 2319-5991 www.ijerst.com

Vol. 15, Issue.4, Dec 2019

Tip finish and blend machining:

The advice proved flexible. The titanium thin-size wall geometry was CNC finished and blended using power MILL machining, which involved a highly cautious 500-1,500 mm/min feed speed with a spindle vessel of 2,000 rpm, and was performed without coolant or robust fixation utilizing the ball's nose cutting system. The milling exhibited short fills from the laser cladding (where not enough material was stored), but it helped resurface and return the blade to its desired form and tolerance otherwise.

Figure 8: Adaptive CNC blending of repaired air foil tip

The inspection capability was originally envisaged as the final inspection phase at multiple points in the processing phases. Early trials gave an insight into the effects of each move in terms of the component accuracy. Experiments were run to see if the part's dimensions changed enough after laser cladding to necessitate rescanning in order to regenerate adaptive pathways and ensure an efficient combination due to thermally-induced distortion, and this was determined based on the significant thermal input in a small thin wall region

INTRODUCTION TO CAD CAM:

The work emphasizes on the use of Computers in the field of production i.e., CAD/CAM. The term CAD/CAM is a shortening of computer-Aided design (CAD) and Computer-Aided manufacturing (CAM). It is the technology concerned with the use of digital computer to perform certain functions in design and production. This technology is moving in the direction of greater integration of design and manufacturing. CAD/CAM will provide the technology base for the computer-integrated factory of the future

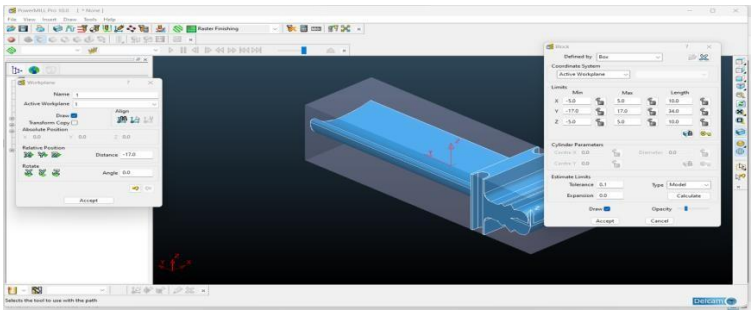

Figure 9: Imported model in CAD CAM Software

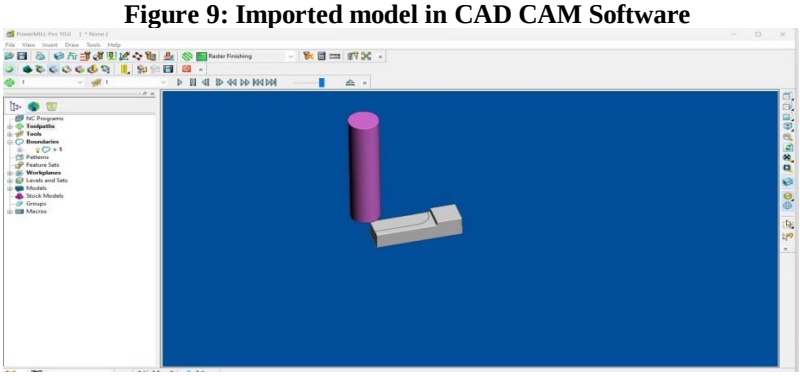

Figure 10: turbine blade tool Analyzation with Inconel material

ISSN 2319-5991 www.ijerst.com

Vol. 15, Issue.4, Dec 2019

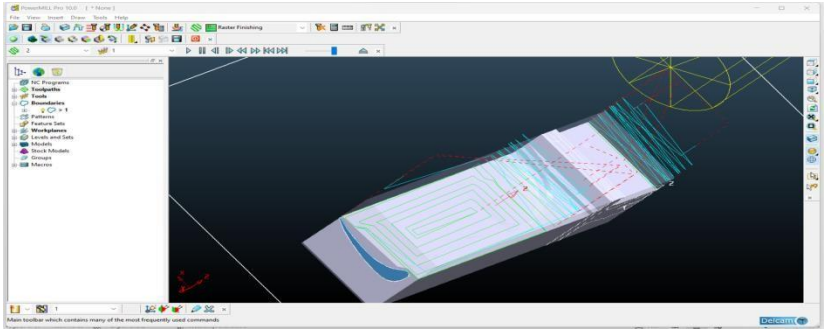

Figure 11: turbine blade optimization process with INCONEL 718 Material

CNC MACHINING PROCESS OF GAS TURBINE BLADES:

Surfaces with complicated geometries are often utilized in mechanical manufacturing to achieve goals including efficiency, aesthetics, and reduced weight. The cutting settings, however, were shown to be the cause of some dimensional and geometric abnormalities. In this study an empirical model of the cutting strength is proposed which is perpendicular to the instruments axis and combines experimental model with analytical models, grouping rigidity and cutting parameters.

3-Axis CNC Machining

3-axis CNC milling is still one of the most popular and widely used machining processes. In 3-axis machining, the workpiece remains fixed and the rotating tool cuts along X, Y and Z axes. This is a relatively simple form of CNC machining, which can manufacture products with simple structure. It is not suitable for processing products with complex geometry or complex components.

Features:

- Most suitable for small size Dia making application
- Basic Machine - Bridgeport three axes Milling Machine
- Retrofitted Axes - X axis - 800 mm, Y axis - 300 mm, Z axis (Knee Axis)- 450 mm
- X, Y, Z axes with Ground Guide -ways with Turbine Coating
- Ball Screws of PMI make-C-3 Class
- Machine with three spindle heads and independent RPM Control
- Spindle speed upto 3500 rpm continuously variable
- Siemens 802-D control with DNC control
- Rapid Traverse Rate of 10 meters/min
- Standard Accessories
- Auto Coolant System
- Gross weight of 2500 kg (appx.)

4.0 RESULTS AND DISCUSSIONS

- Steady-state thermal analysis involves assessing the equilibrium state of a system subject to constant heat loads and environmental conditions.
- The simplest form of steady-state analysis is linear steady-state analysis in which input parameters, such as material properties, are prescribed independent variables.

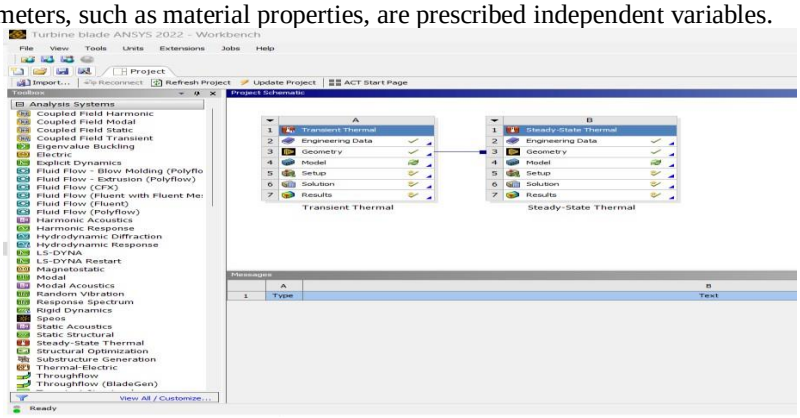

ISSN 2319-5991 www.ijerst.com

Vol. 15, Issue.4, Dec 2019

Figure 12: ANSYS Layout

Inconel 718 Material Study state thermal analysis:

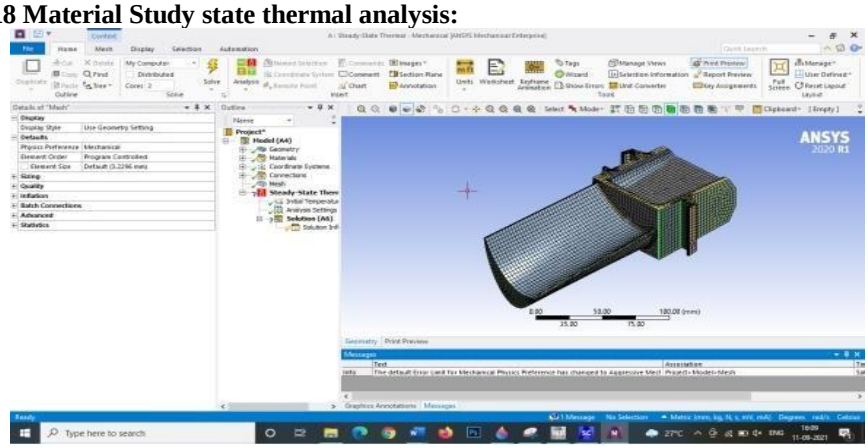

Figure 13: Meshed view

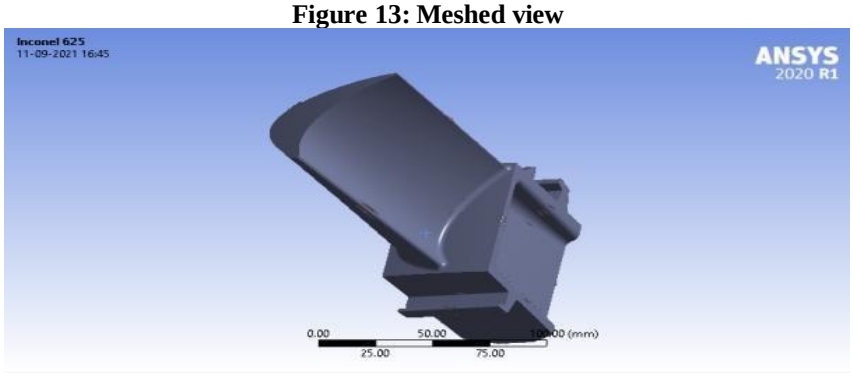

Figure 14: Material property assignment for the blade with layer thickness of 350 µm

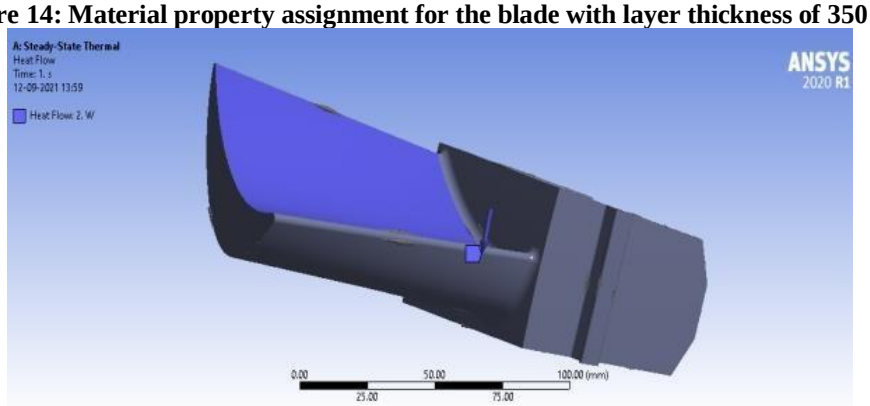

Figure 15: Directional heat flow on blade profile

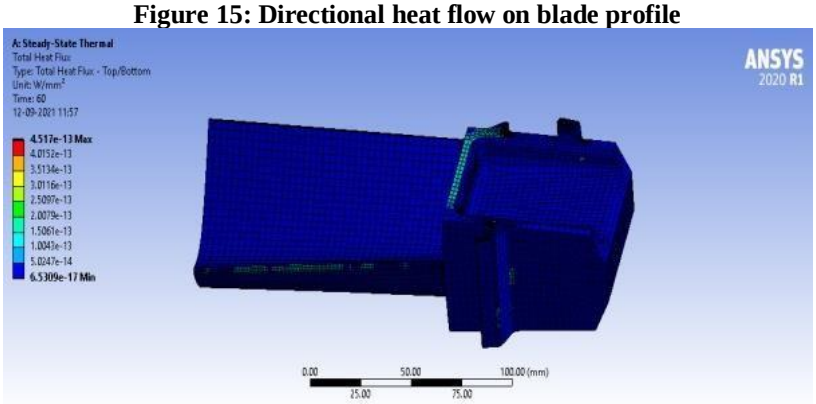

Figure 16: Heat flux area

ISSN 2319-5991 www.ijerst.com

Vol. 15, Issue.4, Dec 2019

Heat flux was found to be largest along the figure's profile and root edges. This demonstrates that high thermal depositions can cause damage, with a damage growth rate of 1.0043E-13.

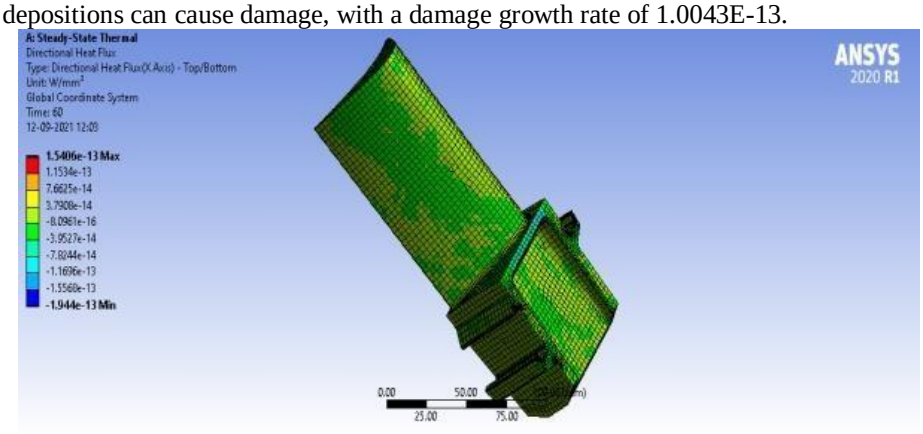

Figure 17: Directional heat flux on top and bottom profiles

The above diagram shows heat transferring from the upper to lower profiles, where it is deposited. The top, concave contour absorbs the most heat, with a maximum value of 3.7908E-14, while the bottom, convex profile absorbs between 3.7908E-14 and -8.0961E-16.

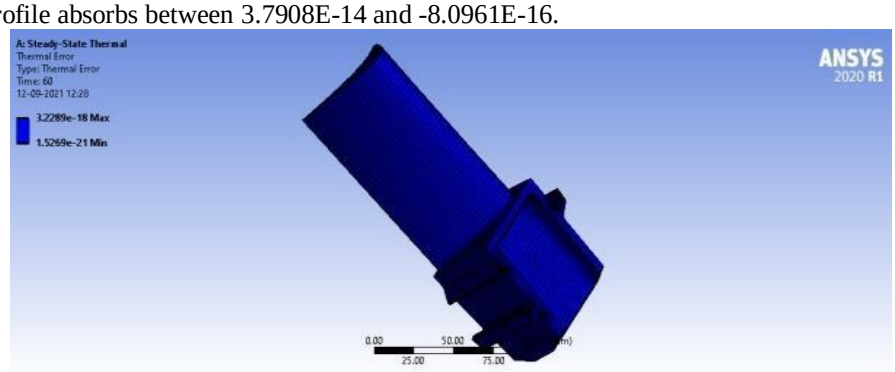

Figure 18: Thermal error

Thermal error varies from 3.2289E-18 to 1.5269E-21. There is a maximum mean error difference of 1.702E-19.

Titanium T6 Material Study state thermal analysis

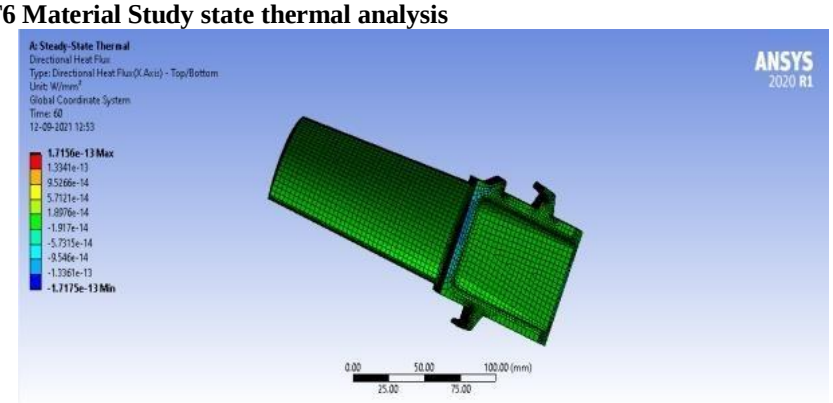

Figure 19: Directional heat flux

The heat is being conducted from the top profile to the lower profile, as depicted in the above image. At a value of 5.7121E-14, the root edge is where the most heat is absorbed.

ISSN 2319-5991 www.ijerst.com

Vol. 15, Issue.4, Dec 2019

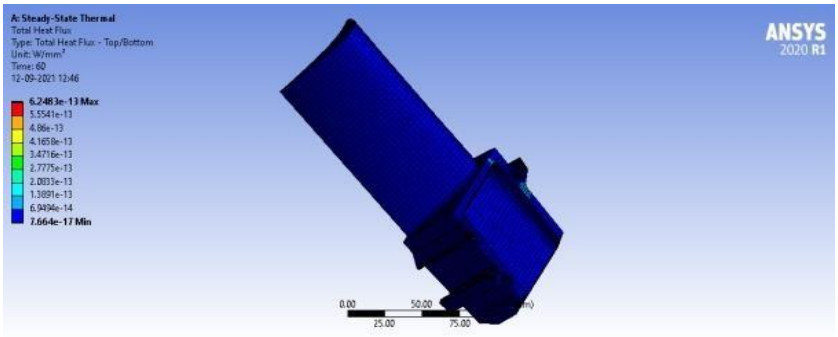

Figure 20: Total heat flux

Maximum heat flux formed near root edges, as seen in the above figure. Extreme heat caused by depositions at a damaging growth rate of 1.3891E-13.

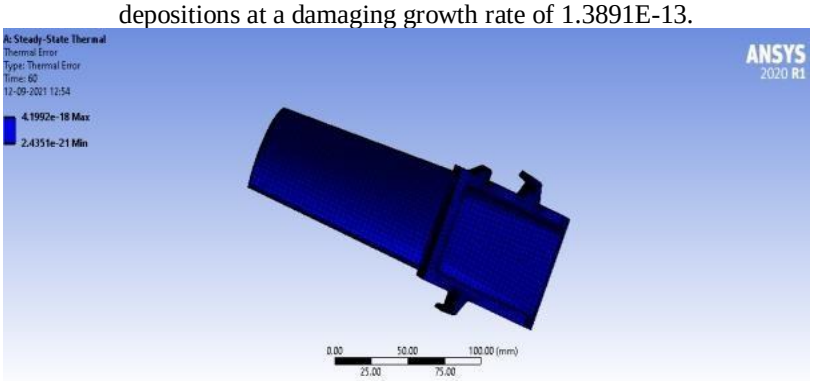

Figure 21: Thermal error

The value of thermal error is varying from 4.1992E-18 to 2.4351E-21. The maximum of mean error difference is 1.7641E-19.

SS316Material Study state thermal analysis

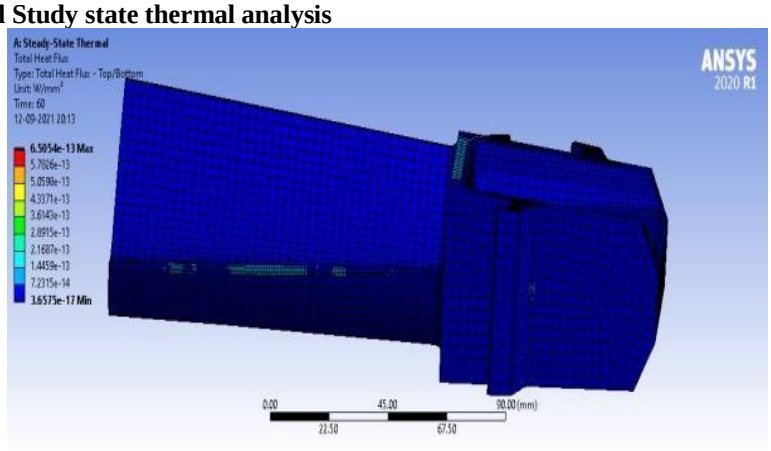

Figure 22: Total heat flux

Maximum heat flow was created along the profile and lean edges, as shown in the above figure. Specifically, the 1.4459E-13 and 4.3371E-13 high thermal depositions at the damaged growth rate.

ISSN 2319-5991 www.ijerst.com

Vol. 15, Issue.4, Dec 2019

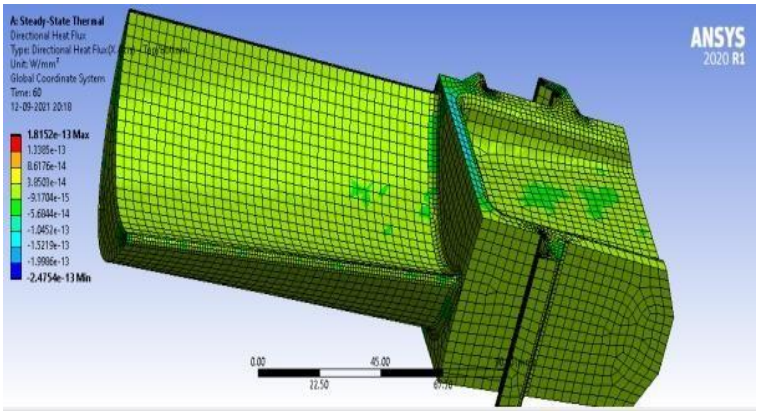

Figure 23: Directional heat flux

Heat is being transferred from the upper to the lower profile, and hot spots have been mapped out above. Maximum heat deposit is -5.6044E-14 at the profile edge, -1.5219E-13 at the lean edge, and 3.6603E-14 at the root edge.

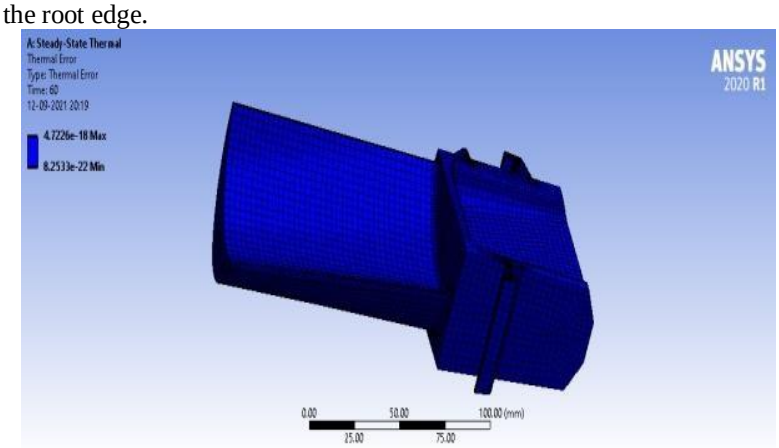

Figure 24: Thermal error

The value of thermal error is varying from 4.7726E-18 to 8.2533E-22. The maximum of mean error difference is 3.4807E-20.

Inconel 718 Material Transient Thermal Analysis:

The process involves measuring the system's response to both static and dynamic boundary conditions. The time required to obtain a steady state temperature and the duration of operation before reaching a critical temperature can be calculated under fixed boundary conditions. Transient analysis can reveal the system's thermal response to time-varying boundary conditions. All temperature changes in this case study were calculated while accounting for a thermal boundary condition of 900^0C ambient.

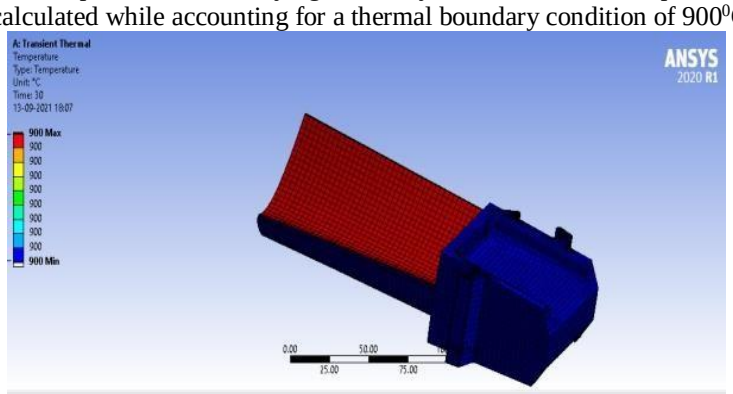

Figure 25: Thermal gradients inside the blade

Constant temperature analysis of the heat flow and directional heat flux under this situation has been performed for the gas turbine environment at 900^0C.

ISSN 2319-5991 www.ijerst.com

Vol. 15, Issue.4, Dec 2019

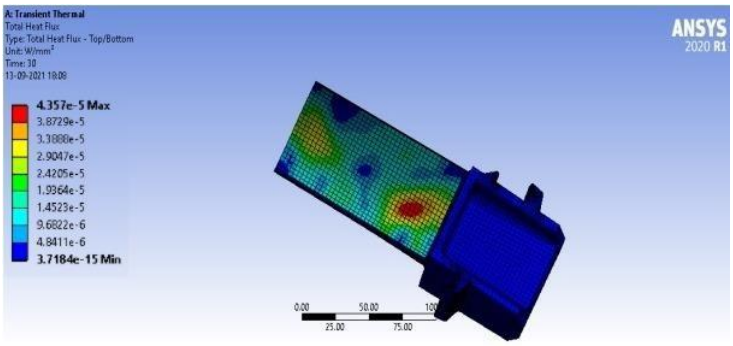

Figure 26: Total heat flux

In the initial environment, the root profile and the tail created the maximum heat flux. The maximum value is shown to be 1.2895E-12.

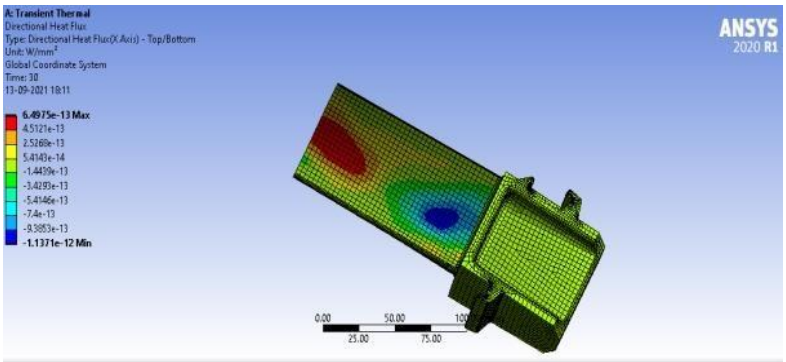

Figure 27: Directional heat fluxes at 900^{0}C

Directional heat flow towards tail in ambient conditions a difference of 6.4975E-13

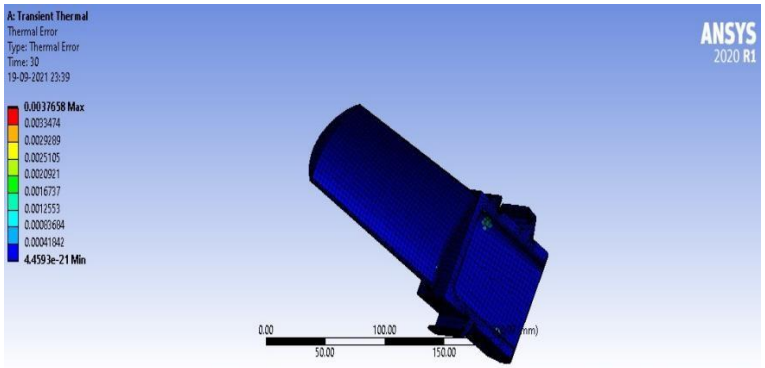

Figure 28: Thermal errors

Model for thermal inaccuracy does not find such fluctuation because input condition is ambient.

Titanium -T6 Material Transient Thermal Analysis:

ISSN 2319-5991 www.ijerst.com

Vol. 15, Issue.4, Dec 2019

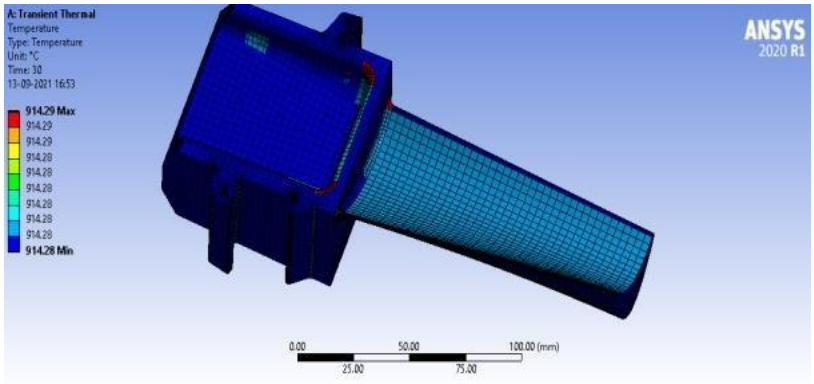

Figure 29: Temperature gradient in blade model

The internal temperature of the model reached 14.280C after being heated by 10000C.Total model analysis temperature deposition at known profile beginning and ending locations

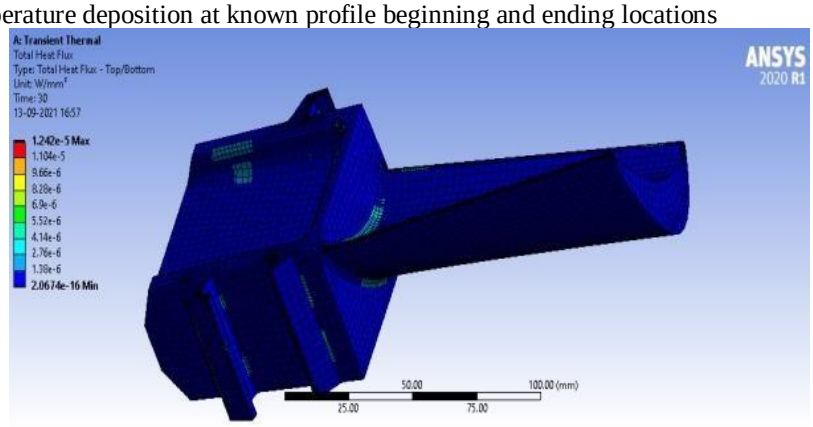

Figure 30: Heat flux

The root profile and root regions are the sites of fluxes. The highest value is 1.242E-5, which is what was measured.

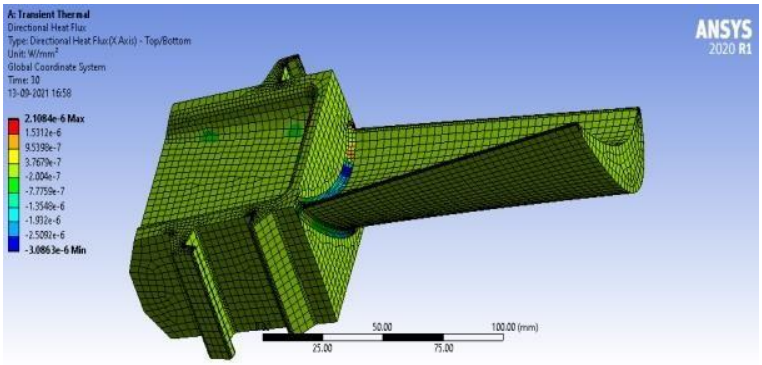

Figure 31: Directional heat flux

The maximal flux contours created at the blade profile's initial root are also visible in the directional heat flux.

ISSN 2319-5991 www.ijerst.com

Vol. 15, Issue.4, Dec 2019

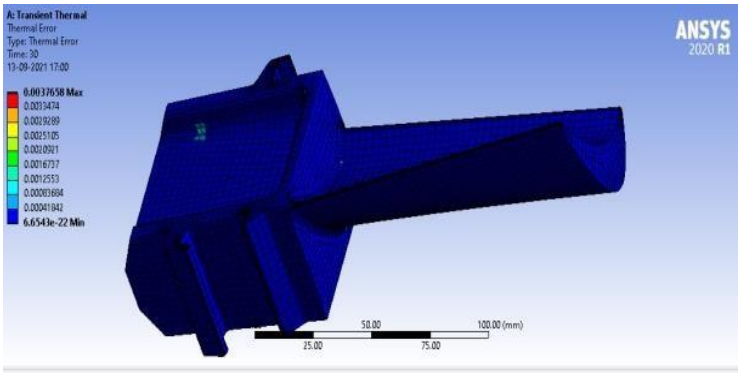

Figure 32: Thermal errors

The differential thermal error observed in the model 3.7658x10-3.

SS 316Material Transient Thermal Analysis

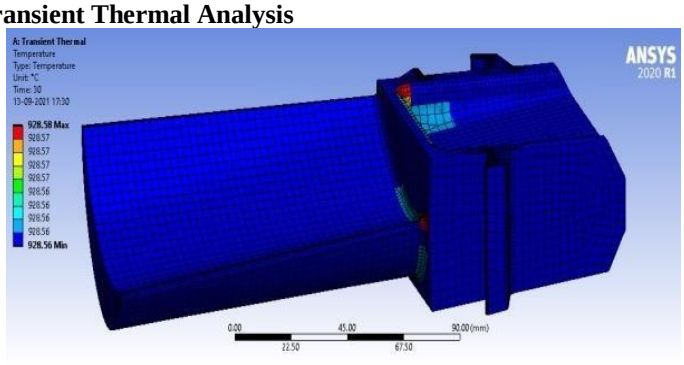

Figure 33: Thermal gradients inside the model

By observing the heat load condition at 1100^0C bottom root profile having a temperature difference of 28.59^0C from the ambient

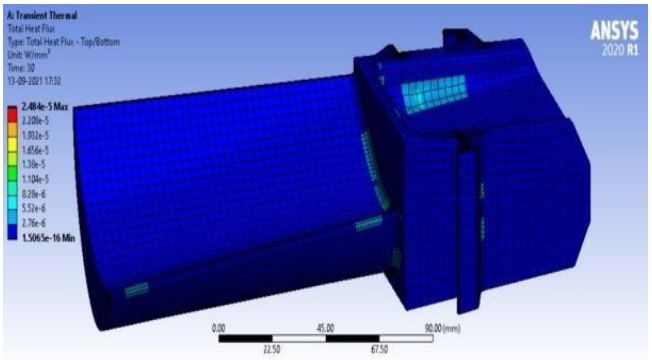

Figure 34: Total heat flux

The heat flux formed at the bottom edge and the root edges.

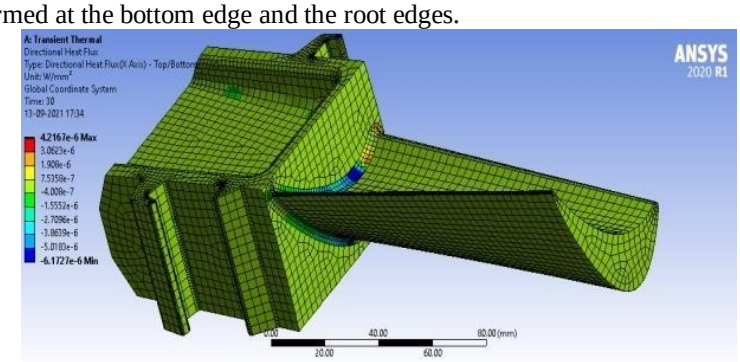

Figure 35: Directional heat flux

ISSN 2319-5991 www.ijerst.com

Vol. 15, Issue.4, Dec 2019

Most of the damage is concentrated at the blade's central stem, where the directional heat flow is shown by flux contours.

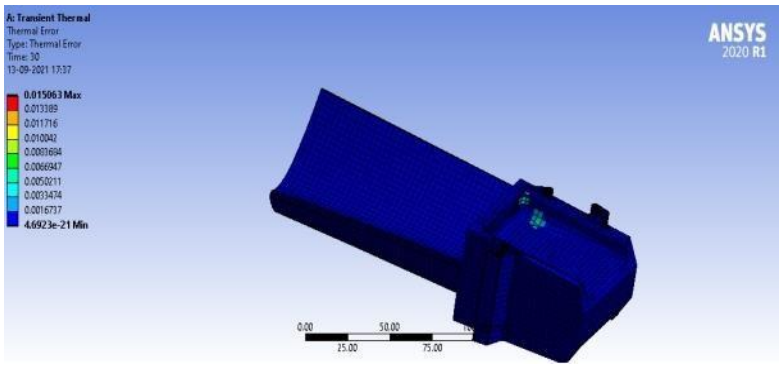

Figure 36: Thermal errors

The value of thermal inaccuracy was observed to increase to 15.063 x 10-3 when compared with ambient conditions.

Inconel 718 materials Directional heat flow transient analysis with 28 MPa Pressure:

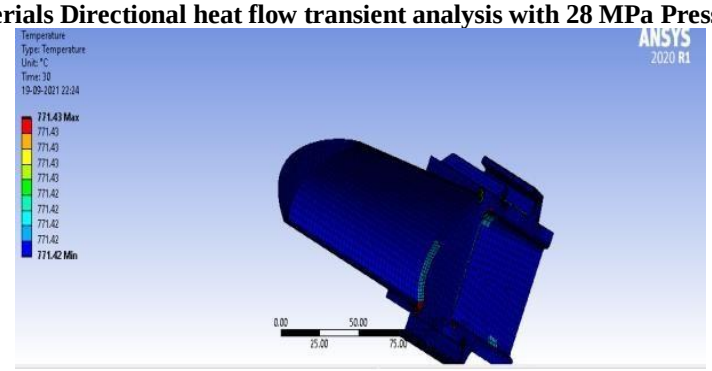

Figure 37: Temperature

The maximum temperature of the blade is 771.43 degrees Celsius with an input pressure of 28 MPa and a gas temperature of 9000C in a turbine ambient temperature of 700^{0}C. Both the blade's edge and its base show maximum temperature contours.

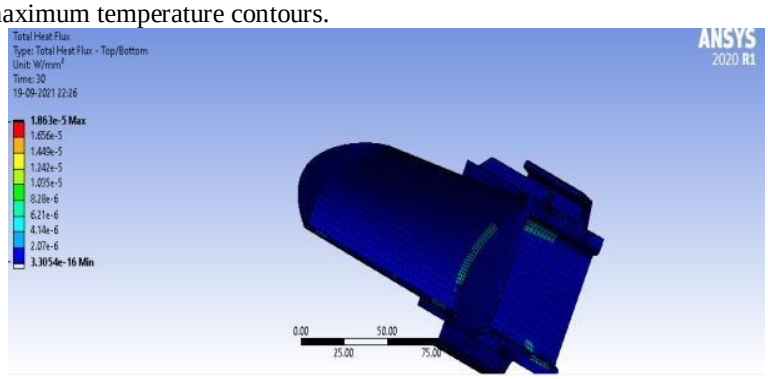

Figure 38: Total heat flux

The highest heat flux of 1.863E-5 is created in the turbine environment at 7000C, when the input pressure is 28MPa and the gas temperature is 900^{0}C.

ISSN 2319-5991 www.ijerst.com

Vol. 15, Issue.4, Dec 2019

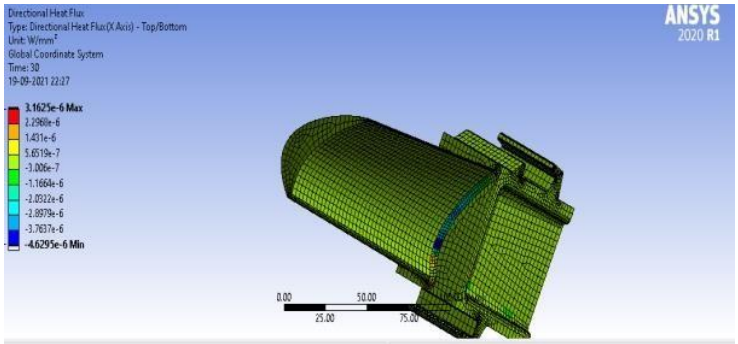

Figure 39: Directional heat flux

When the gas temperature is 9000C and the input pressure is 28MPa, the directional heat flux in the turbine environment is 3.1625E-6. Both the total root and the edge profile show evidence of a directed heat flux developing.

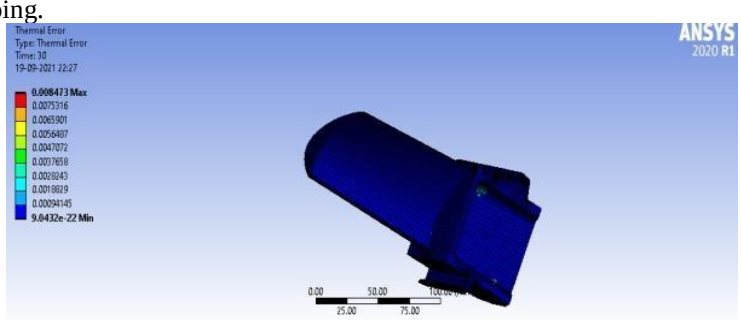

Figure 40: Thermal error

The thermal inaccuracy is 8.473E-3 at 28 MPa input pressure, 9000 C gas temperature, and 700^0C turbine ambient temperature.

Titanium -T6 materials Directional heat flow transient analysis with 28 MPa Pressure:

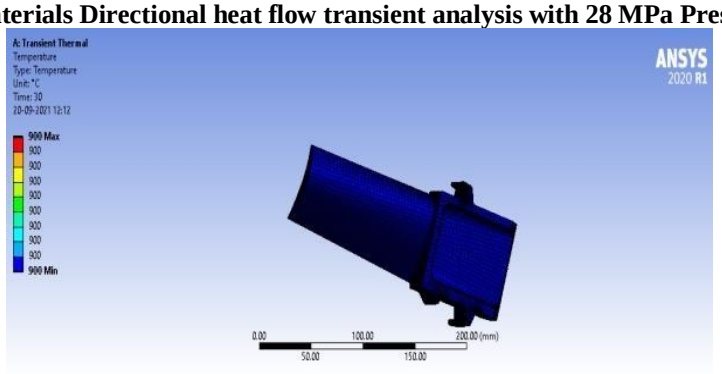

Figure 41: Temperature

Blade temperature is 9000C with an input pressure of 28MPa and gas temperature of 10000C, with the turbine ambient temperature being 700^0C.

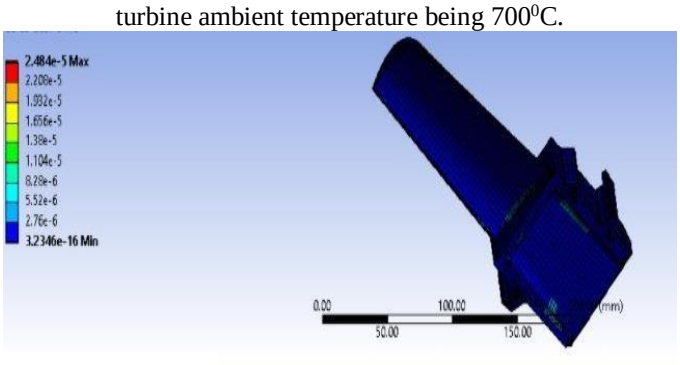

ISSN 2319-5991 www.ijerst.com

Vol. 15, Issue.4, Dec 2019

Figure 42: Total heat flux

When the gas entering the turbine has a temperature of 1000^0C, and the ambient temperature of the turbine is 700^0C, the entire heat flow is observed on the blade's whole profile, but more strongly at the starting point of the root, the tail, and the edge profile. Maximum heat flux as a whole is 1.6372E-12

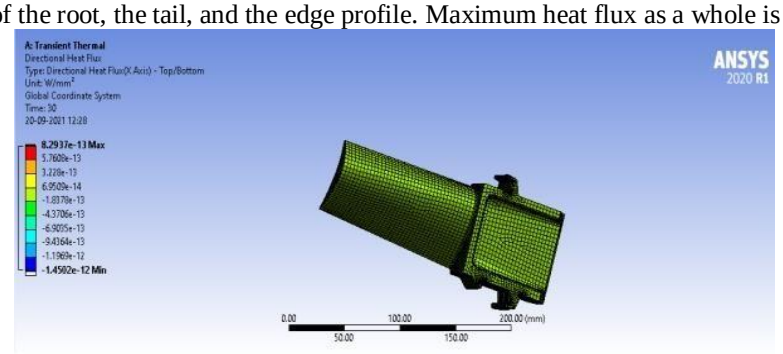

Figure 43: Directional heat flux

At an input pressure of 28 MPa, gas temperature of 1000^0C, and turbine environment temperature of 700^0C, directional heat flow is seen across the whole blade profile, with a maximum at the end of the tail and a minimum at the root (-8.2937E-13 and -1.4502E-12, respectively).

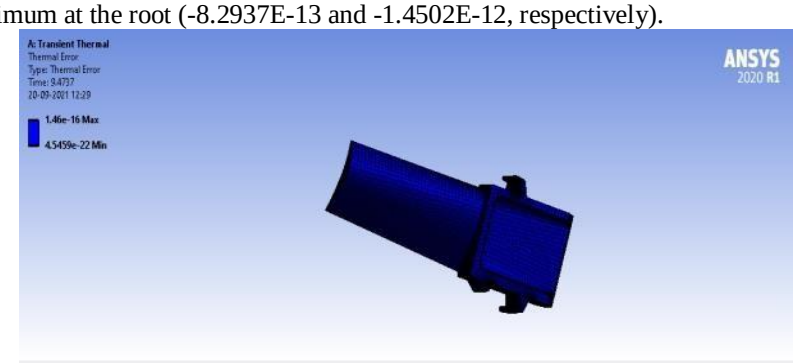

Figure 44: Thermal error

Maximum thermal error is 1.46E-16 at 28MPa input pressure, 10,000°C gas temperature, and 7,000°C turbine ambient temperature.

SS316 materials Directional heat flow transient analysis with 28 MPa Pressure:

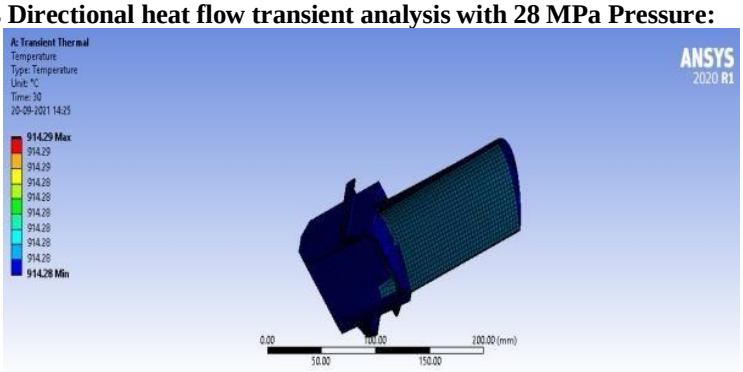

Figure 45: Temperature

The blade temperature climbed by 914.28 degrees Celsius at an input pressure of 28MPa and a gas temperature of 1100^0C in a turbine environment temperature of 700^0C, with a maximum temperature of 914.29 degrees Celsius observed at the root edges.

ISSN 2319-5991 www.ijerst.com

Vol. 15, Issue.4, Dec 2019

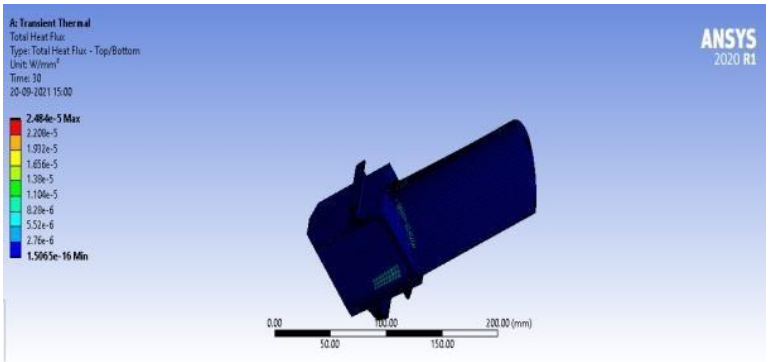

Figure 46: Total heat flux

Maximum total heat flux is seen at the turbine's root edges with an input pressure of 28 MPa, gas temperature of 1100^{0}C, and turbine environment temperature of 700^{0}C. The highest possible number is 2.208E-5.

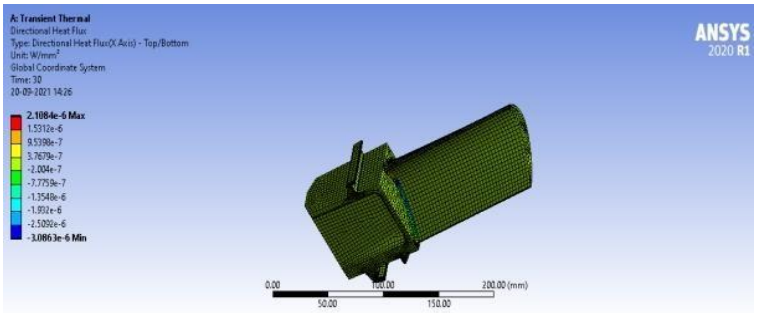

Figure 47: Directional heat flux

Root edge directional heat flow is increased at 28MPa input pressure, 1100^{0}C gas temperature, and 7000C turbine environment temperature. For a complete profile, the directional heat flux is -2.004E-7. The maximum value is 2.1084E-6.

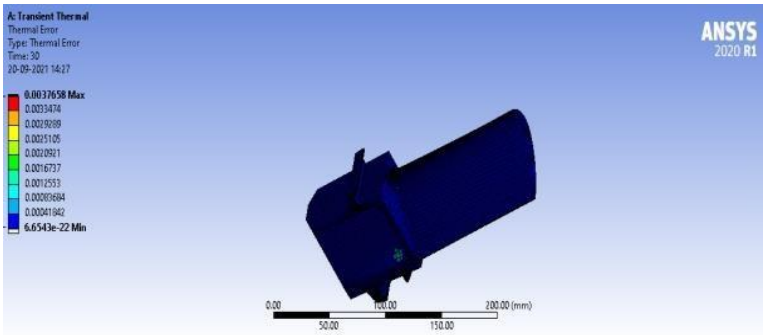

Figure 48: Thermal error

When the input pressure is 28MPa, the gas temperature is 1100^{0}C, and the turbine environment temperature is 700^{0}C, the maximum thermal error formed is 3.7658E-3.

Table 2: Total heat flux at different conditions

Materials	Steady State Thermal	Transient Thermal	Transient Thermal at Pressure 28MPa
Inconel 718	4.517e-13	0.484e-5	1.863e-5
Titanium -T6	6.2483e-13	1.242e-5	2.484e-5
SS316	6.5054e-13	2.984e-5	4.357e-5

ISSN 2319-5991 www.ijerst.com

Vol. 15, Issue.4, Dec 2019

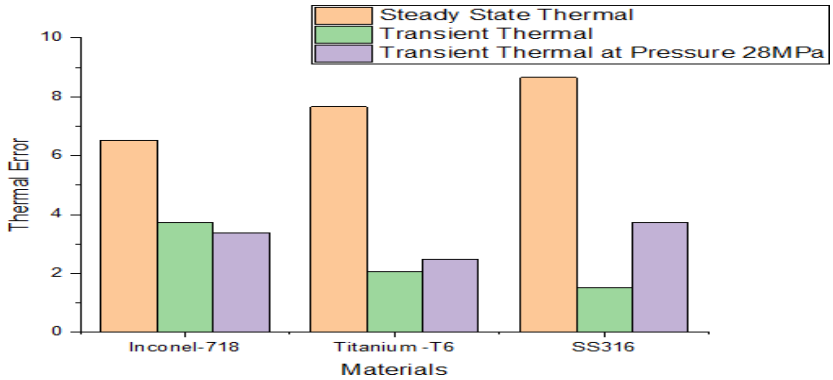

Graph: 1: Total heat flux Maximum

Table 3: Directional heat flux at different conditions

Materials	Steady State Thermal	Transient Thermal	Transient Thermal at Pressure 28MPa
Inconel 718	1.540	1.523	3.162
Titanium -T6	1.715	2.108	4.216
SS316	2.8152	4.216	8.108

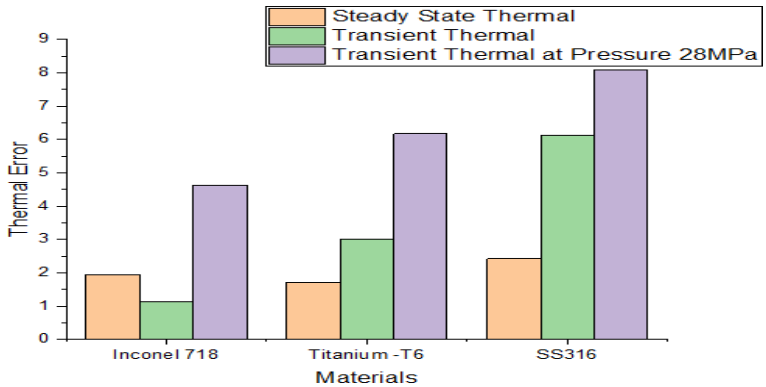

Graph 2: Directional heat flux maximum

Table 4: Thermal error at different conditions

Materials	Steady State Thermal	Transient Thermal	Transient Thermal at Pressure 28MPa
Inconel 718	3.228	4.236	0.847
Titanium -T6	4.199	3.7658	1.596
SS316	4.722	3.4563	3.765

ISSN 2319-5991 www.ijerst.com

Vol. 15, Issue.4, Dec 2019

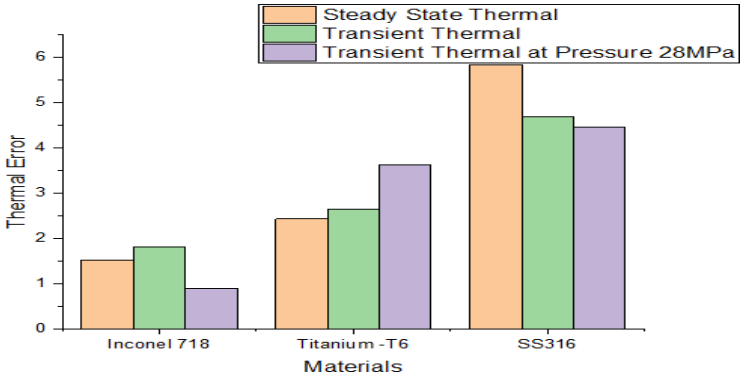

Graph 3: Thermal Error Maximum

Conclusions:

One of a gas turbine engine's most crucial parts is the turbine blade. High pressures, high temperatures, and strong centrifugal forces all hinder the performance of blade materials under climatic circumstances.In steady state, there is very little change in the total heat flow; however, under transient and transitory thermal conditions at 28 MPa of pressure, the heat flux increases quickly as temperature rises, as the graph illustrates. As temperature rises, the heat flow increases quickly in steady state thermal conditions, but it also increases in transient thermal conditions at a pressure of 28 MPa. This is seen in Graph 1.

- As graph 2 illustrates, the directional heat flow varies relatively little in a steady state but quickly increases with temperature in a transient and transitory thermal condition at pressure of 28 MPa.
- under a steady state, the thermal error varies quickly; however, under transient and transient thermal conditions at pressures of 28 MPa, the thermal error progressively increases as temperature rises, as shown in graph 3.

Lastly It is shown in the simulation that mild damage is occurring all the way up to Inconel 718. However, it will also have better yield and elastic strength values, which will result in less stress being placed on the blade. Furthermore, Inconel 718 is seen to have superior mechanical qualities at elevated temperatures in contrast to titanium T6 and SS316.

It is recommended for future endorsement that the coating be raised without changing the profile shape based on the findings of the simulation. By altering the hot gas's input pressure, a variant model analysis was conducted; concave profiles are detected for the majority of the temperature contours based at the leaving edge and heat fluxes. Model study indicating that the blade analysis findings might change depending on the pressure and vector directions can be examined for potential future improvements. A good advantage with this study's restriction to coating process parameters and deposit thickness might be beneficial for further investigation.

ISSN 2319-5991 www.ijerst.com

Vol. 15, Issue.4, Dec 2019

REFERENCES:

1. S. Rani S, A.K. Agrawal, V. Rastogi, "Failure analysis of a first stage IN738 gas turbine blade tip cracking in a thermal power plant". Case Studies in Engineering Failure Analysis, pp. 1–10, 2017.
2. A.M. Kolagar, N. Tabrizi, M. Cheraghzadeh, M.S. Shahriari, Failure analysis of gas turbine first stage blade made of nickel-based superalloy. Case Studies in Engineering Failure Analysis. 2017 Apr;8: 61–8.
3. Mirhosseini AM, Adib Nazari S, Maghsoud Pour A, Etemadi Haghighi S, Zareh M, "Failure analysis of first stage nozzle in a heavy-duty gas turbine", Engineering Failure Analysis, 2020 Jan;109:104303.
4. B. Swain, P. Mallick, S. Patel, R. Roshan, S.S. Mohapatra, S. Bhuyan, et al., "Failure analysis and materials development of gas turbine blades", Materials Today: Proceedings [Internet]. 2020 Apr 3
5. H. Kazempour-Liasi, A. Shafiei, Z. Lalegani, "Failure Analysis of First and Second Stage Gas Turbine Blades", J Fail Anal and Preven, Vol. 19, No. 6, pp. 1673–82, 2019.
6. R. Wang, B. Zhang, D. Hu, K. Jiang, H. Liu, J. Mao, et al., "Thermomechanical fatigue experiment and failure analysis on a nickel-based superalloy turbine blade", Engineering Failure Analysis, Vol. 102, pp. 35–45, 2019.
7. L. Umamaheswararao, Dr. K. Mallikarjunarao. “Design and analysis of a gas turbine blade by using FEM”, ISSN: 2278-621X, Vol. 4 Issue 4 November 2014 published by International Journal of Latest Trends in Engineering and Technology (IJLTET).
8. P.V.Krishnakanth, G.Narasa Raju, R D V. Prasad, R. Saisrinu. “Structural & Thermal Analysis of Gas Turbine Blade by Using F.E.M”, ISSN 2278 – 0882, Volume 2 Issue2 pp 060-065 May 2013 published by International Journal of Scientific Research Engineering & Technology (IJSRET).
9. Ahmed Abdulhussein Jabbar, A. K. Rai, P. Ravinder Reedy & Mahmood Hasan Dakhil. “Design and analysis of gas turbine rotor blade using finite element method”, ISSN(P): 2249-6890; ISSN(E): 2249-8001, Vol. 4, Issue 1, Feb 2014, 73-94, International Journal of Mechanical and Production Engineering Research and Development (IJMPERD).
10. Murali K and B Rambabu. “Design and Fatigue Analysis of Turbine Rotor Blade by Using F.E.M”, ISSN No: 2348-4845, Volume No: 2 (2015), Issue No: 4 (April), International Journal & Magazine of Engineering, Technology, Management and Research.
11. Sindhu N L1, Dr. N Chikkanna Design and Analysis of Gas Turbine Blade International Journal for Research in Applied Science & Engineering Technology (IJRASET) Volume 5 Issue VI, ISSN: 2321-9653, June 2017.